

Crack growth resistance of hybrid fiber reinforced cement composites

N. Banthia ^{*}, N. Nandakumar

Department of Civil Engineering, The University of British Columbia, Vancouver, BC, Canada V6T 1Z4

Received 6 November 2000; accepted 4 June 2001

Abstract

Crack propagation in cement-based matrices carrying hybrid fiber reinforcement was studied using contoured double cantilever beam (CDCB) specimens. Influence of fiber type and combination was quantified using crack growth resistance curves. It was demonstrated that a hybrid combination of steel and polypropylene fibers enhances the resistance to both nucleation and growth of cracks, and that such fundamental fracture tests are very useful in developing high performance hybrid fiber composites. The influence of number of variables which would otherwise have remained obscured in normal tests for engineering properties become apparent in the fracture tests. The paper emphasizes the desired durability characteristics of these composites and discusses their current and future applications.

© 2002 Elsevier Science Ltd. All rights reserved.

Keywords: Crack growth; Hybrid fiber; Cement composites

1. Introduction

The low tensile strength and poor fracture toughness of cement-based materials are serious shortcomings that not only impose constraints in structural designs, but also affect the long-term durability of structures. In this regard, the benefits of fiber reinforcement in improving the fracture toughness, impact resistance, fatigue endurance and energy absorption capacity of concrete are well known. Fibers resist the nucleation of cracks by acting as stress-transfer bridges, and once cracks nucleate, fibers abate their propagation by providing crack tip plasticity and increased fracture toughness. Reinforcement of concrete with fibers, however, still remains a science in its infancy, and ideas are still evolving towards assessing the characteristics of an optimal fiber system.

One idea gaining much attention lately is that of *fiber hybridization*. In a hybrid, two or more different types of fibers are rationally combined to produce a composite that derives benefits from each of the individual fibers and exhibits a synergistic response. The precise ways in

which various fibers should be combined to produce a synergistic response, however, are not understood.



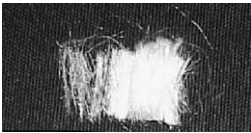

Broadly one can divided the hybrid composites into two categories. In the first, fibers different in sizes are combined. The idea of such dimensional hybrids follows directly from concrete itself where particles of different sizes are combined to achieve a dense packing and dimensional stability. Typically, one would combine large macro-fibers that provide toughness at large crack openings with fine micro-fibers that reinforce the mortar phase and enhance the response prior to or just after cracking. Micro-fibers are also expected to improve the pull-out response of the macro-fibers, and thus produce composites with high strength and toughness. Dimensional hybrids using steel fiber have been previously studied [1], but have not yet been fully optimized.

The second type of hybrid composites involves combining fibers of similar sizes but different moduli. One example would be combining high modulus steel or carbon fibers with low modulus polypropylene fiber. The high modulus fiber, if properly bonded, would attain its optimal reinforcing capability at small to medium crack openings. The low modulus fiber, such as polypropylene, on the other hand, would develop its full reinforcement capability only at large crack openings. In

^{*}Corresponding author. Tel.: +1-604-822-9541; fax: +1-604-822-6901.

E-mail address: banthia@civil.ubc.ca (N. Banthia).

Table 1
Properties of steel and polypropylene fibers

Fibers	Geometry	Average diameter (mm)	Length (mm)	Tensile strength (MPa)	Young's modulus (GPa)
 Xorex steel	Continuously crimped	1.0	50	828	212
 Novotex steel	Flattened ends with round shaft	1.0	50	1150	200–210
 Stealth	Monofilament polypropylene	6 Denier ^a	12	375	3.5
 MD	Fibrillated polypropylene	230–2600 Denier ^a	11–20	375	3.5

^a Weight of a 9000 m long fiber in grams.

combination, therefore, these fibers are expected to produce a composite with high toughness over a wide range of crack openings. Our understanding of these composites is also only rudimentary.

The purpose of the work reported here was to combine the benefits of the above two types of hybrids. Large fibers of steels were combined with fine fibers of polypropylene such that benefits of both differing fiber sizes as well as differing fiber moduli were simultaneously achieved.

Generally, to fully understand and maximize the reinforcement efficiency of fibers in a given matrix, fiber-matrix pull-out tests are performed on macro-fibers. Unfortunately, for hybrids involving macro-fibers of steel and secondary micro-fibers of polypropylene, single fiber pull-out tests are not appropriate as they involve a pre-cracked matrix, and any influence of the secondary fiber on the fracture resistance itself of the matrix remains obscured. Here, a somewhat different approach was adopted. Cracks were allowed to propagate under a near constant stress-intensity factor in an idealized double cantilever beam specimen carrying both steel macro-fiber and polypropylene micro-fiber. Micro polypropylene fi-

bers were thus allowed to contribute both to the processes of matrix cracking as well as to steel fiber pull-out.

2. Experimental program

2.1. Materials and mixes

Two types each of steel and polypropylene fibers were investigated. Properties of Xorex fiber, Novotex fiber, Stealth (ST) fiber and MD fiber are reported in Table 1. The fiber combinations and details of composites are given in Table 2.

The matrix chosen was a mortar matrix with the following proportions: cement:water:sand (by weight) = 1:0.45:1. This mix developed a compressive strength of 41 MPa at 28 days.

2.2. Crack growth studies

Fig. 1 shows a schematic of the contoured double cantilever beam (CDCB) specimen that was adopted for characterization of the crack growth resistance. As seen,

Table 2
Fiber combinations investigated

Primary steel fiber	Secondary fiber volume fraction (%)	
	ST	MD
Xorex, 50 mm	0	0
	0.1	0
	0.2	0
	0	0.1
	0	0.2
Novotex, 1050	0	0
	0.1	0
	0.2	0
	0	0.1
	0	0.2

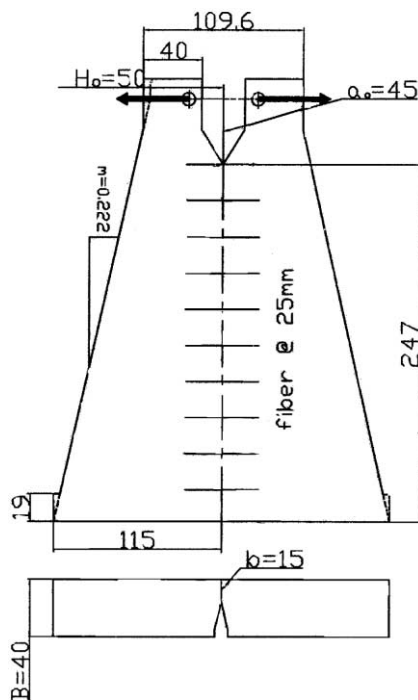


Fig. 1. Schematic of a CDCB specimen and fiber layout.

steel fibers were placed perpendicular to the direction of crack growth at a spacing of 25 mm and the fresh mortar matrix was poured while the mould was externally vibrated. The cementitious mix used was either a plain mortar without a secondary polypropylene fiber, or a mortar with 0.1 or 0.2% by volume of the MD or the ST fiber (see Table 2). In a parallel series, steel fibers were eliminated and the crack growth resistance of the mortar itself with 0, 0.1 or 0.2% by volume of the MD or the ST fiber was investigated.

In a test, the load was applied vertically at a cross-arm rate of 0.1 mm/min (Fig. 2) that resulted in a horizontal opening load (OL) magnitude of which was

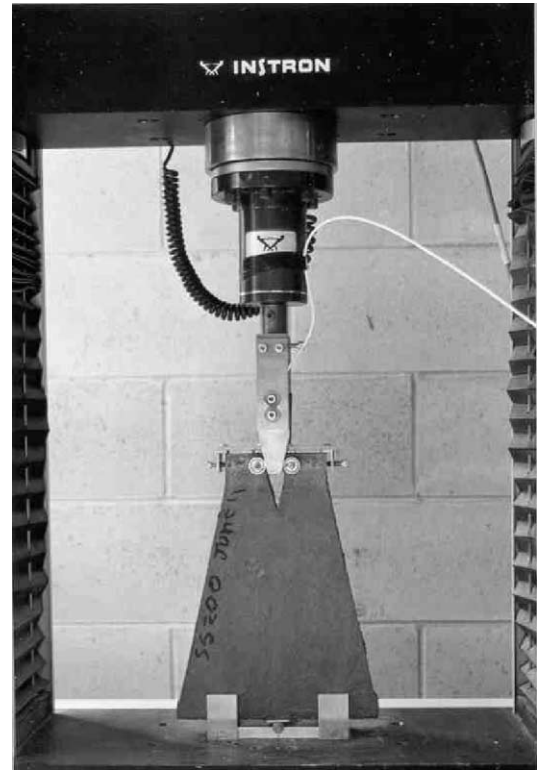


Fig. 2. A CDCB specimen under load.

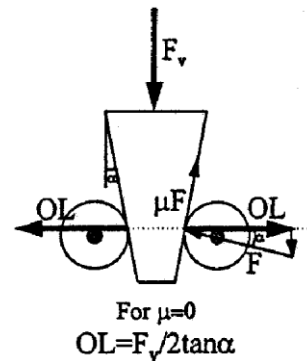


Fig. 3. Vertical load resolved in a CDCB to obtain the crack OL.

calculated by resolving loads as shown in Fig. 3 [2–4]. Clearly, the specimen was subjected to a vertical load in addition to the horizontal crack OL. In order to be able to ignore the vertical component of the applied load, the angle of the wedge was kept low at 15°. While the coefficient of friction μ (Fig. 3) was ignored, clearly it increased as the angle of the wedge was decreased. The crack mouth opening displacement (CMOD) was measured using a clip gauge displacement transducer fixed at the level at which the OL acted on the specimen. The applied load and the CMOD data were acquired using a digital data acquisition system running at 5 Hz. The OL–CMOD curves were further analyzed to obtain the

crack growth resistance (R -curves) as described in Appendix A. The purpose of choosing a contoured geometry is to achieve a constant rate of change of compliance with crack growth [$\partial C/\partial a = \text{constant}$] such that this parameter is independent of the crack length [2].

3. Results and discussion

Averaged Opening Load vs. CMOD curves are given in Figs. 4 and 5 for the Xorex fiber and in Figs. 6 and 7 for the Novotex fiber. The OL vs. CMOD curve for the control mortar without any reinforcement are also given in these figures.

Notice a significant improvement in the OL–CMOD curves due to the presence of steel fibers. Notice also the distinct differences in the shapes of curves obtained for the Xorex fiber as opposed those obtained for the Novotex fiber. This clearly implies that these fibers impart very different reinforcement mechanisms to the cementitious matrix – a fact that often remains obscured in the single fiber pull-out tests or the flexural toughness tests. In the case of the Novotex fiber, the curves attained a peak load followed by a sudden drop in the load carrying capacity. In the case of the Xorex fiber, on the other hand, the curves depict hardening with an

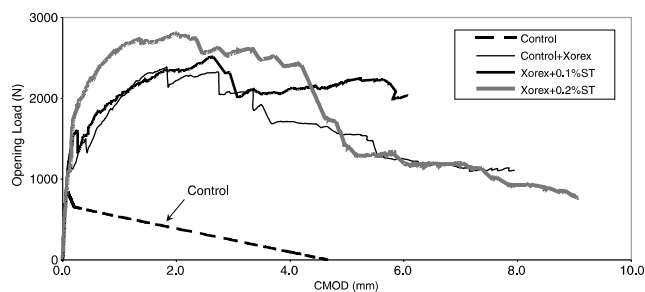


Fig. 4. OL vs. CMOD plots for Xorex fiber with various fractions of the ST secondary fiber.

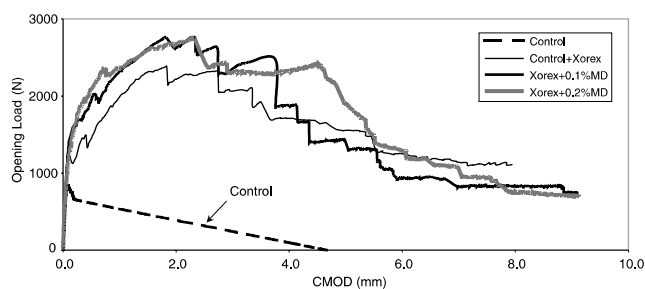


Fig. 5. OL vs. CMOD plots for Xorex fiber with various fractions of the MD secondary fiber.

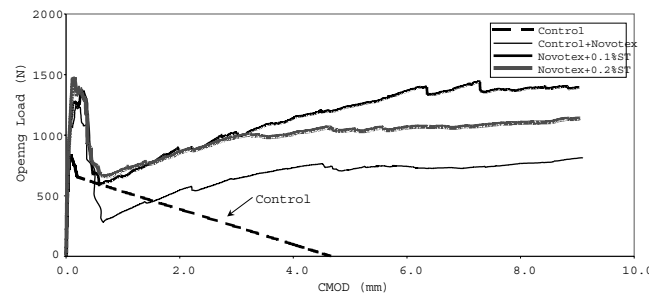


Fig. 6. OL vs. CMOD plots for Novotex fiber with various fractions of the ST secondary fiber.

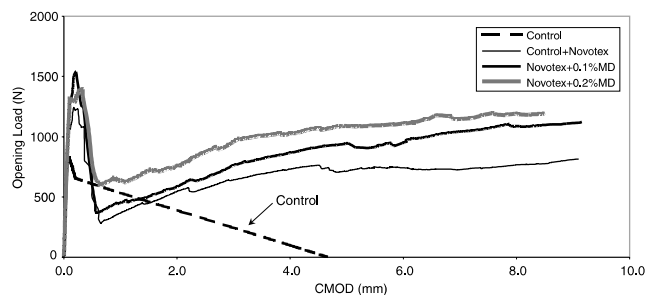


Fig. 7. OL vs. CMOD plots for Novotex Fiber with various fractions of the MD secondary fiber.

increase in the crack-opening displacement, and generally much more stable curves are obtained. Notice also the general enhancement in the performance of the two steel fibers due to the presence of the secondary fiber.

The curves in Figs. 4–7 were analyzed for fracture energy G_f values, defined as the area under the OL–CMOD curve divided by the projected cracked area. These quantities are plotted in Fig. 8(a) for the specimens without the steel fiber and in Fig. 8(b) for specimens with steel fibers. The G_f values are of a greater significance for specimens with steel fibers as the calculation of this quantity is valid only for cases where a stable fracture is obtained. Notice in Fig. 8(a), that the presence of the secondary fibers enhanced the fracture energy requirements. Notice from Fig. 8(b) that the incorporation of a secondary fiber was effective in enhancing the G_f values.

Curves in Figs. 4–7 were further analyzed and converted to R -curves (Appendix A) that are shown in Figs. 9 and 10 for the Xorex fiber and in Figs. 11 and 12 for the Novotex fiber. It is clear from the R -curves that incorporating a nominal volume fraction of the secondary polypropylene fiber in the matrix can derive significant advantages and that the ST fiber is more effective than the MD fiber. While synergy between the two fibers is already apparent in the hybrids, further optimization attempts are clearly warranted.

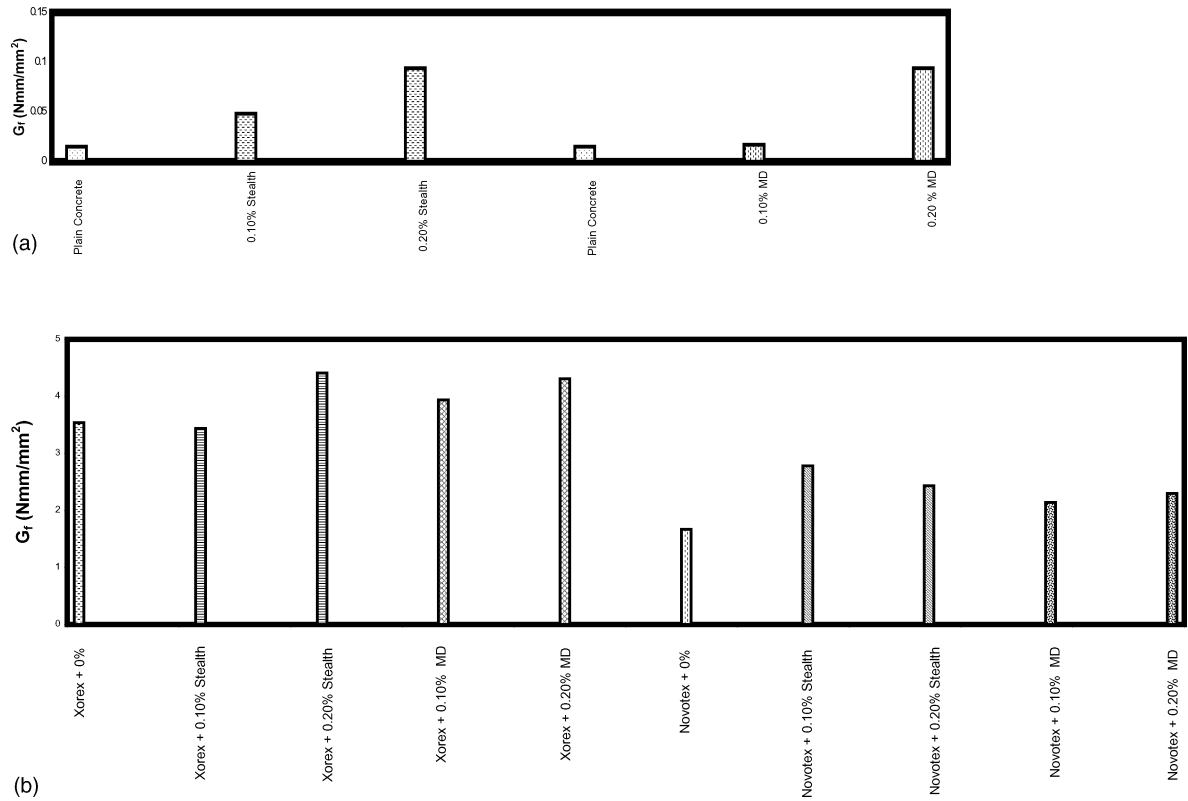


Fig. 8. (a) Fracture energy G_f values plotted for mortars with only the secondary fibers; (b) fracture energy G_f values plotted for mortars with both primary and secondary fibers.

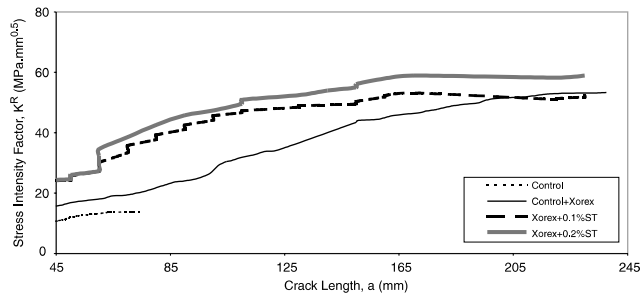


Fig. 9. R -curves for Xorex fiber with various fractions of the ST secondary fiber.

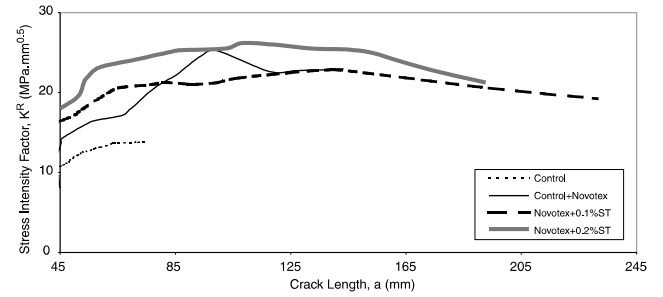


Fig. 11. R -curves for Novotex fiber with various fractions of the ST secondary fiber.

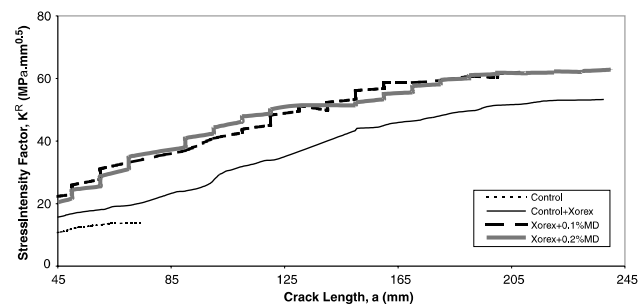


Fig. 10. R -curves for Xorex fiber with various fractions of the MD secondary fiber.

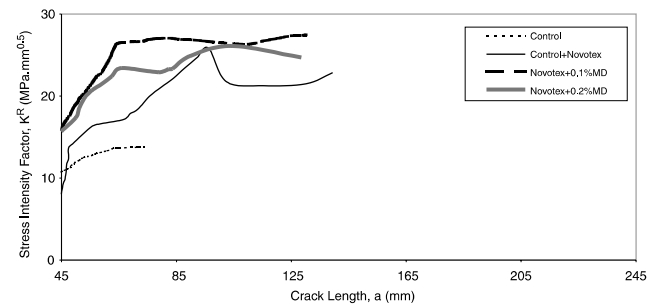


Fig. 12. R -curves for Novotex fiber with various fractions of the MD secondary fiber.

4. Applications of hybrid composites and further research

Hybrid fiber reinforced cement-based composites, especially the ones with a high fracture toughness, are potentially useful in slabs on grade, shotcrete and thin pre-cast products like roofing sheets, tiles, curtain walls, cladding panels, I- and L-shaped beams, permanent forms, etc. Given that the secondary fiber of a polymeric material will enhance the resistance to shrinkage cracking, the hybrid composites may prove significantly useful as a material for repairs and retrofit. Some of these composites can be made good conductors of electricity, which makes them a candidate for static free floors, lightning arresters, etc. Given the high fatigue endurance and impact resistance anticipated from the hybrid composites, their use in machine foundations, earthquake resistant structures, blast shelters, etc., can also prove to be beneficial. Numerous non-structural applications of hybrid fiber reinforced composites may also be suggested including their use by the electrical and electronics industries.

5. Conclusions

1. Crack growth studies based on fundamental fracture tests are useful in characterization and optimization of high performance hybrid fiber reinforced composites.
2. The use of a secondary polypropylene micro-fiber even at nominal dosage rates appears to be highly effective in enhancing the efficiency of deformed steel fibers in concrete. Among the two polypropylene fibers tested, the ST monofilament fiber appears to be more effective than the MD fiber.

Acknowledgements

The continued support of the Natural Sciences and Engineering Research Council of Canada is gratefully acknowledged. Thanks are also due to Synthetic Industries, Chattanooga, for supplying the fibers.

Appendix A. Determination of K_R -curves for a CDCB specimen

A.1. Compliance of the CDCB specimen

The expression for the compliance of the CDCB specimen (Fig. 1) was obtained using the strength of materials approach.

If one assumes that one arm of the CDCB is a simple cantilever beam with a constant section BH and a span

equal to the crack length a (Fig. 1), the compliance C of the specimen is given by

$$C = 2\Delta/P = \frac{\text{CMOD}}{P}$$

$$= \frac{24}{EB} \int_0^a \frac{x^2}{H^3} dx + \frac{6(1+\nu)}{EB} \int_0^a \frac{1}{H} dx.$$

The two terms on the right-hand side are the contribution to the compliance from bending and shear deformations, respectively. The constant height of the beam is assumed to be equivalent to the mean height of the corresponding contoured cantilever beam H_c , that is

$$H_c = \frac{H_0 + H_a}{2}, \quad H_a = H_0 + ma.$$

Therefore

$$H_c = H_0 + \frac{ma}{2}.$$

The additional deflection due to the rotation of the assumed “built-in” end of the cantilever beam is accounted for by using a longer crack length in the calculation of the compliance term due to the bending deformation. Using a rectangular DCB, Mostovoy et al. [5] determined experimentally that the rotational effect was equivalent to considering a crack of length of about $a + 0.6H_c$.

Assuming $\nu = 0.2$, the expression for the compliance of the CDCB specimen is a function of crack length can then be rewritten as

$$C = \frac{24}{EB} \left\{ \frac{(a + 0.6H_c)^3}{3H_c^3} + \frac{0.3a}{H_c} \right\}. \quad (\text{A.1})$$

A.2. Calculation of the effective crack length

The elastic modulus of the material is calculated using the initial compliance C_i obtained from the experimental

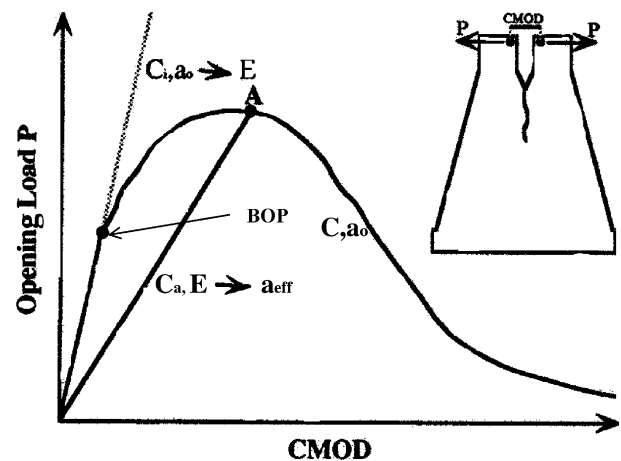


Fig. 13. Typical OL vs. CMOD curve obtained from a CDCB test.

OL (P) vs. $CMOD$ curve (Fig. 13) and the initial crack length a_o . The initial compliance is defined as,

$$C_i = \left. \frac{CMOD}{P} \right|_{\text{at the first non-linearity point (BOP)}}.$$

Using Eq. (A.1),

$$E = \frac{24}{C_i B} \left\{ \frac{(a + 0.6H_c)^3}{3H_c^3} + \frac{0.3a}{H_c} \right\}. \quad (A.2)$$

After the BOP, sub-critical crack growth occurs extent of which can be determined from the observed increase in compliance. The elastically equivalent crack length corresponding to the increase is usually referred to as the effective crack length, a_{eff} .

Ignoring permanent deformations, the compliance of the specimen at any point A in the non-linear region is given by

$$C_A = \frac{CMOD_A}{P_A}.$$

Using the values of E and C_A , a_{eff} is computed using an iteration scheme.

A.3. Calculation of the stress intensity at the crack tip

The Mode I stress intensity factor (K_I) is calculated using the LEFM equation for a CDCB specimen which is based on derivation by Srawley and Gross [6]. This equation is

$$K_I^2 = \frac{P^2}{B^2 H^3} \eta^2 (a^2 + 1.4aH + 0.5H^2) \quad (A.3)$$

in which $\eta = 3.1$ for a slope $m = 0.222$ and H is the beam height at the distance a from the point of loading, H_a .

It must be noted that in Eq. (A.3) one B (in the B^2 term) holds for the beam height while the other B represents the cracked width. Thus, because the specimen contains a side-groove along its mid-plane, one of the B has to be changed for the cracked width b . Finally, to account for slow crack growth, the stress intensity is therefore calculated using the effective crack length a_{eff} . The equation [2] in its final form is then

$$K = \left\{ \frac{9.6P^2}{BbH^3} (a_{\text{eff}}^2 + 1.4a_{\text{eff}}H_a + 0.5H_a^2) \right\}^{1/2}. \quad (A.4)$$

References

- [1] Banthia N, Bindiganavile V. Development and application of hybrid fiber reinforced cement composites for thin repairs. ACI, Conc Int, submitted.
- [2] Genois I. Fracture resistance of micro fiber reinforced cement composites. MASc Thesis, The University of British Columbia, 1995, 155 p.
- [3] Banthia N, Genois I. Pitch-based carbon fiber reinforced cement composites. In: Proceedings of 2nd International University – Industry Workshop on Fiber Reinforced Concrete, Toronto, The University of British Columbia, 1995, p. 213–28.
- [4] Banthia N, Genois I. Controlled crack growth tests for optimization of micro-fiber reinforced cement composites. In: Vipulanandan, editor. ACI, Special Publication on Concepts of Fracture Mechanics Applied to Concrete, to appear.
- [5] Mostovoy S, Crosley PB, Ripling EJ. Use of crack-line-loaded specimens for measuring plane-strain fracture toughness. J Mater 1967;2(3):661–81.
- [6] Srawley JE, Gross B. Stress Intensity Factors for Crack Line Loaded Edge-Crack Specimens. Mater Res Stand 1967;7(4):155–62.